rescence was collected at right angles to the laser excitation beam and detected by a Hamamatsu R928 photomultiplier tube. Discrimination against scattered light was accomplished by a combination of filters (Corion LS-750-S) and a Spex (Edison, NJ) model 1680A monochromator. The dye-laser output was polarized by a Glan-Laser linear polarizer and passed through a set of three Fresnel rhombs before arriving at the sample. Two of the Fresnel rhombs are rotated together around the propagation axis of the excitation light, which allows the vector of the linearly polarized light to be rotated before it enters the third (stationary) rhomb. The dye laser wavelength, its intensity, and the fluorescence intensity measured by the photomultiplier were processed by a Compaq 386 microcomputer.

17. The transition probability for two-photon absorption from a single source, $W^{(2)}$, can be written as

$$W^{(2)} \propto I^2 \left| \sum_n \frac{\langle \psi_f|\mu|\psi_n\rangle\langle\psi_n|\mu|\psi_i\rangle}{\Delta E_{ni} - \hbar\omega_r} \right|^2$$

where I is the intensity of the incident laser beam, ψ_n is the virtual intermediate state, ψ_i and ψ_f are the initial and final states, respectively, μ is the electric dipole moment operator, ΔE_{ni} is the energy of the virtual state, $\hbar$ is Planck's constant divided by 2π, and ω_r is the frequency of the incident radiation. Thus, the transition probability is proportional to the square of the intensity of the incident laser beam. More generally, the transition probability for an n-photon process is proportional to I^n [S. H. Lin, Y. Fujimura, H. J. Neusser, E. W. Schlag, *Multiphoton Spectroscopy of Molecules* (Academic Press, Orlando, FL, 1984), chap. 4].

18. In one-photon spectroscopy, the absorption cross section, σ, for randomly oriented molecules is related to the transition dipole

$$\sigma \propto |\boldsymbol{\lambda} \cdot \mu_{fi}|^2$$

where $\boldsymbol{\lambda}$ is the unit polarization vector of the absorbed photon. Because $\lambda \cdot \lambda^* = 1$, there is no polarization information contained in the observed transition. In two-photon spectroscopy, however, the absorptivity is given by

$$\langle\delta\rangle = |\boldsymbol{\lambda} \cdot \mathbf{S}_{fi}^{ab} \cdot \boldsymbol{\kappa}|^2$$

where $\boldsymbol{\kappa}$ and $\boldsymbol{\lambda}$ are the polarization vectors of the two absorbed photons and $\mathbf{S}_{fi}^{ab}$ is the two-photon transition tensor. The polarization ratio, Ω, may be expressed in terms of the absorptivity in circular and linear polarizations, δ_{cir} and δ_{lin}, respectively

$$\Omega = \frac{\langle\delta_{cir}\rangle}{\langle\delta_{lin}\rangle}$$

If two photons of the same energy are used, then the polarization ratio is bounded by $0 \leq \Omega \leq 3/2$.

19. P. R. Monson and W. M. McClain, *J. Chem. Phys.* **53**, 29 (1970); W. M. McClain, *ibid.* **55**, 2789 (1971); M. A. Nasciemento, *Chem. Phys.* **74**, 51 (1983).
20. M. D. Hopkins *et al.*, *J. Am. Chem. Soc.* **109**, 408 (1987); M. D. Hopkins, V. M. Miskowski, H. B. Gray, *ibid.* **110**, 1787 (1988).
21. Strictly speaking, this energy gap should be measured from the electronic origins of the two transitions, but the absence of vibrational fine structure in the two-photon spectrum precludes location of the 0–0 vibronic component.
22. From the effective overlap of 0.1 [as determined from the oscillator strength of the $\delta\delta^*$ transition (*11*)] and the spectroscopically determined ΔW and K from this work, the 34% ionic character of the ground state increases significantly to 68% in the zwitterionic excited state (J. F. Harrison, unpublished results).
23. M. D. Hopkins, T. C. Zietlow, V. M. Miskowski, H. B. Gray, *J. Am. Chem. Soc.* **107**, 510 (1985); F. A. Cotton, J. L. Eglin, B. Hong, C. A. James, *ibid.* **114**, 4915 (1992); F. A. Cotton, J. L. Eglin, B. Hong, C. A. James, *Inorg. Chem.* **32**, 2104 (1993).
24. F. A. Cotton and X. Feng, *J. Am. Chem. Soc.* **115**, 1074 (1993).
25. X. Zhang, M. Kozik, N. Sutin, J. R. Winkler, in *Electron Transfer in Inorganic, Organic, and Biological Systems*, J. R. Bolton, N. Mataga, G. McLendon, Eds. (American Chemical Society Advances in Chemistry Series no. 228, Washington, DC, 1991), pp. 247–264.
26. J. Hubbard, *Proc. R. Soc. London Ser. A* **276**, 238 (1963).
27. C. M. Partigianoni, I.-J. Chang, D. G. Nocera, *Coord. Chem. Rev.* **97**, 105 (1990); C. M. Partigianoni *et al.*, in *Mixed Valency Systems: Applications in Chemistry, Physics, and Biology*, K. Prassides, Ed. (NATO Advanced Study Institutes Series C no. 343, Kluwer Academic, Dordrecht, Netherlands, 1991), pp. 91–106; C. M. Partigianoni, C. Turró, T.-L. C. Hsu, I.-J. Chang, D. G. Nocera, in *Photosensitive Metal-Organic Systems*, C. Kutal and N. Serpone, Eds. (American Chemical Society Advances in Chemistry Series no. 238, Washington, DC, 1993), pp. 147–163; D. G. Nocera, in *The 30th Anniversary of the Quadruple Bond*, R. A. Walton, Ed. (Journal of Cluster Science no. 5, Plenum, New York, 1994), pp. 185–209.
28. Supported by the National Science Foundation under grants CHE-9100532 (D.G.N.) and CHE-9204136 (G.E.L.).

15 March 1994; accepted 3 June 1994

Antibody-Mediated Bacteriorhodopsin Orientation for Molecular Device Architectures

Koichi Koyama,* Naoto Yamaguchi, Tsutomu Miyasaka

A rational method for constructing highly oriented films of purple membrane (PM) has been established by using two kinds of bispecific antibodies with different antigen-binding sites, one binding to a specific side of bacteriorhodopsin and the other to a phospholipid hapten. A hapten monolayer deposited on a metal electrode was treated with a bispecific antibody solution and incubated with a PM suspension to produce a highly oriented PM film, as confirmed by electron microscopy in which an immunogold labeling technique was used. This antibody-mediated PM monolayer was then used in the construction of a light-sensing photoelectric device. A comparison of the two incorporated PM monolayers showed that highly efficient photocurrents were produced by the PM monolayer whose unidirectionally oriented cytoplasmic surface faces the electrode.

Bacteriorhodopsin (bR) is the sole protein found in the PM in *Halobacterium halobium*. Uniformly oriented bR molecules in PM perform unidirectional pumping of protons from the cytoplasm to the extracellular space during the photocycle, thereby forming an electrochemical gradient across the membrane. The three-dimensional structure and photocyclic reaction of bR have been well elucidated by Henderson and co-workers (*1*) and Khorana and co-workers (*2*).

The photocycle of bR and its rapid optical change (*3*) exhibit versatile photophysical functions in vitro; these functions can provide components that are critically important in the design of molecular electronic devices (*4*) and optical memories (*5*). We have verified that a PM-immobilized liquid-junction photocell exhibits differential electrical responsivity to light intensity, a function characteristic of vertebrate photoreceptors (*6*). One potential application for this responsivity is in the manufacture of an artificial retina that could detect and process optical information in a manner closely approximating certain visual functions (*7*).

In bR-based photoelectric devices, a truly integrated unidirectional—and thus highly efficient—electric response can be obtained only when the bR molecules have a nonrandom orientation. In this respect, efforts thus far to control the orientation of PM have included methods such as dispersion at the air-water interface, on charged membrane surfaces, in an electric field, and so forth (*8*). However, in most cases PM orientation is deduced on the basis of the direction and intensity of the photoelectric response of the PM monolayer after it has been incorporated into a device system. This sort of indirect approach frequently leads to conclusions that are confusing or contradictory (*8*).

The reason for this ambiguity is that no direct method has been devised that provides a precise means for controlling and determining the orientation of PM fragments. We have established an immunogold labeling technique that provides a highly accurate means of determining the ratio of orientation of PM sheets (*9*).

We describe a method to establish the perfect reorientation of bR through use of bispecific (BS) antibodies that simultaneously recognize both a phospholipid hapten and a specific side of the bR molecule. Our antibody technique is used to clarify the effect of bR orientation on bR-generated photoelectric events and to conclusively demonstrate the inherent advantages that the ability to precisely control PM orientation holds for the design of molecular devices.

N-(2,4-Dinitrophenyl)aminocaproyl phosphatidylethanolamine (DNP-cap PE,

Ashigara Research Laboratories, Fuji Photo Film Co. Ltd., Minamiashigara, Kanagawa, 250-01, Japan.

*To whom correspondence should be addressed.

obtained from Avanti Polar Lipids, Alabaster, Alabama) was selected as an amphipathic hapten phospholipid. This phospholipid has been used by Uzgiris and Kornberg (*10*) to form a two-dimensional monolayer. An antibody to DNP [immunoglobulin G1 (IgG1)], a monoclonal antibody to the hapten site of the phospholipid (2,4-dinitrophenyl group, DNP), was produced by immunization of mice with 2,4-dinitrobenzene sulfonic acid conjugated to keyhole limpet hemocyanin (KLH).

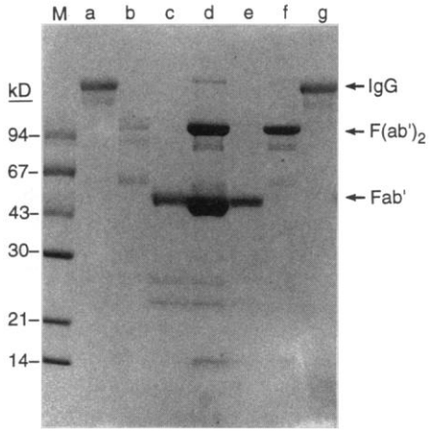

Fig. 1. Steps leading to formation of a BS antibody by SDS–polyacrylamide gel electrophoresis analysis. Lanes a and g, antibody C3-2 or N7-3 and antibody to DNP, respectively; lanes b and f, digested antibodies to $F(ab')_2$ derived from their intact antibodies; lanes c and e, Fab′ reduced with dithiothreitol; lane d, a BS antibody reassociated with Fab′ from C3-2 or N7-3 and from antibody to DNP; lane M, prestained molecular size markers. The obtained BS antibody was purified by high-performance liquid chromatography.

Mice were immunized with peptide-KLH conjugates (*11*) to obtain monoclonal antibodies specific for each side of the bR molecule. Using this procedure, we obtained two antibodies: C3-2 (IgG1), which recognizes a COOH-terminal portion of bR, and N7-3 (IgG2a), which recognizes an NH_2-terminal portion of bR. The epitope and the specificity of the antibodies have been established as described (9). The BS antibodies were prepared by modification of the method of Brennan *et al.* (*12*). As shown in Fig. 1, each of the resulting antibodies was digested with pepsin to obtain an $F(ab')_2$ fragment, which was then reduced with dithiothreitol and reacted with an Ellman's reagent for protection of the mercapto groups. The resulting antibody to DNP Fab′ fragment was chemically reassociated with antibody to bR fragments (derived from C3-2 or N7-3) to yield BS antibodies to DNP-C3-2 and DNP-N7-3, respectively.

To examine the effectiveness of the BS antibody, we prepared a monolayer array of PM oriented on the array of two kinds of BS antibodies and evaluated its degree of orientation with the immunogold labeling technique. A $CHCl_3$ solution of dimyristoyl phosphatidyl choline containing 7% hapten phospholipid (DNP-cap PE) was, under a controlled surface pressure of 30 mN/m, applied on a surface of pure water in a Langmuir film balance to form a monolayer, and the hapten monolayer was deposited onto an electron microscope grid. The grids were treated for 30 min at 37°C with an aqueous solution containing the above-prepared BS antibody to DNP-C3-2 or to DNP-N7-3 (100 μg/ml), respectively, and incubated with a PM suspension (0.4 mg/ml) isolated from the S-9 strain of *H. halobium* with the conventional method (*13*). Each grid-deposited monolayer film was treated with a 0.1% solution of bovine serum albumin to prevent nonspecific adsorption of a gold-labeled antibody on the grid surface in the absence of PM fragments. In the final step, the grid was then incubated with a solution containing an N7-3-Au conjugate (*14*) that recognizes the extracellular surface of PM only. After platinum-shadowing treatment, the grids were observed under an electron microscope (Fig. 2, A and B). A randomly oriented PM monolayer film spontaneously adsorbed on a grid is included here as a reference (Fig. 2C).

The PM monolayer treated with BS antibody to DNP-C3-2 was almost completely covered with gold particles (≥85%) (Fig. 2A), whereas the PM monolayer treated with BS antibody to DNP-N7-3 was devoid of labeling (≤5%) (Fig. 2B). In both cases, the orientation of the PM monolayer was precisely defined. In the first case, the cytoplasmic surface of the PMs was exclusively directed toward the substrate, as indicated by the total covering with gold particles. In the second case, the cytoplasmic surface was inversely directed, as evidenced by the lack of labeling. These results show that the properties of BS antibodies can be harnessed to precisely control the orientation of the PM monolayer.

We next examined the photoelectric response of these antibody-mediated PM films. A sandwich-type photoelectric device (6) was used to obtain a photocurrent response from the PM monolayers. A con-

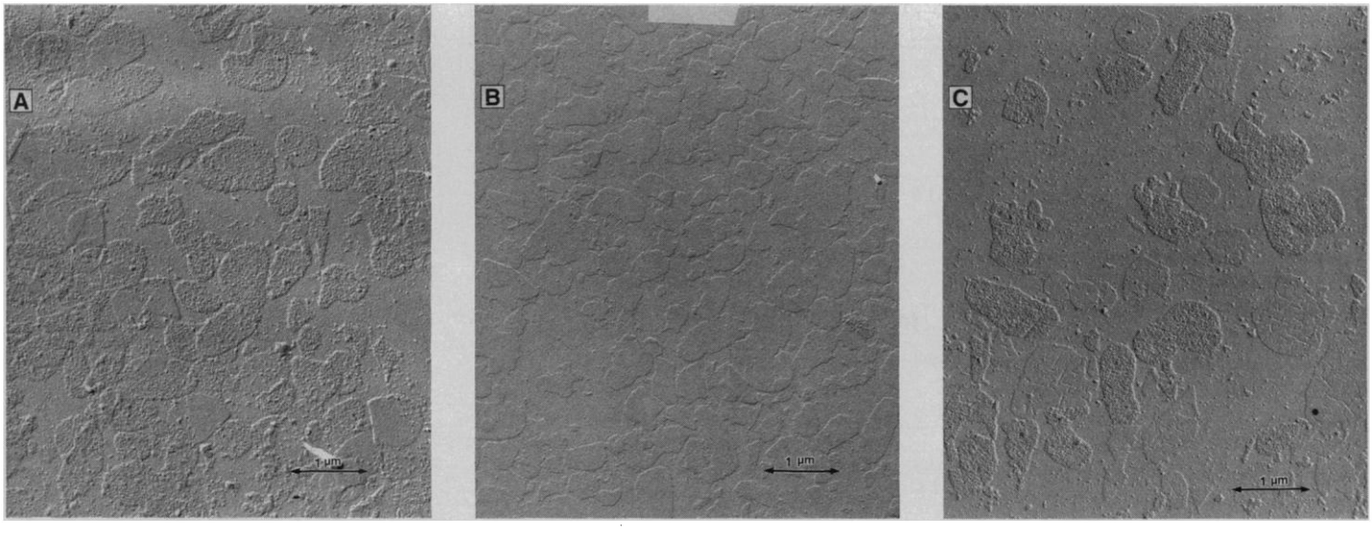

Fig. 2. Surface morphology of PM films as observed by electron microscopy. (**A**) The cytoplasmic side of PM fragments treated with BS antibody to DNP-C3-2 faces the grid surface. (**B**) The extracellular side of PM fragments treated with BS antibody to DNP-N7-3 faces the grid surface. (**C**) Random orientation of PM fragments adsorbed spontaneously on a grid.

ductive SnO_2 electrode that captures the charge displacement current of bR served as a common substrate for the PM monolayer. As described above, the cytoplasmic and extracellular sides of the PM monolayer were oriented toward the electrode (substrate) by using, respectively, the BS antibodies to DNP-C3-2 and DNP-N7-3.

Visible light irradiation of the PM film caused the production of photocurrent signals with characteristic differential response profiles; the direction of the flow of electrons is always rectified from the electrode to electrolyte side. A comparison of the photocurrent signals obtained from the three sources, the two antibody-mediated PM monolayer films and the randomly oriented reference (LB film), is shown in Fig. 3. Exactly the same light intensity was used with all three samples to eliminate the influence of photocurrent, which has a linear relation to light intensity (6).

The peaks of the transient photocurrents produced after the onset of light irradiation indicate the response strength of each of the tested PM monolayers. The most intense response was produced by the sample with the cytoplasmic (COOH-terminal) side of PM directed to the electrode (SnO_2), whereas the weakest response was produced by the sample oriented in the opposite direction. As expected, a moderate response was produced by the randomly oriented sample (LB film), although no antibody layers are inserted between the electrode and PM. Because the response mechanism in this device does not involve electron transfer between electrode and PM, and photocurrent is induced electrostatically through charge displacement within an assembly of bR molecules, the influence of a separating layer (hapten and antibodies) is assumed to be less significant (*15*).

An important finding is that the electric response, which corresponds to displacement of a positive charge toward the electrode surface, is maximal when the cytoplasmic side is oriented to the electrode side. This result implies that the positive-charge displacement contributing to the electric response is inverse to the direction of the proton transfer. A similar relation has been postulated for PM-immobilized dry photocells (*16*). Apparently, on the basis of our experimental evidence, the primary event of vectorial charge transfer in the bR photocycle should occur in a direction opposite to that of proton pumping, which occurs in a time range far later than the initial structural change (*17*).

A rectified photocurrent still exists when the PM orientation is random. This result indicates an electrochemical interfacial effect that externally controls, through an electrostatic field developed in the double layer, the efficiency of charge displacement through the suppression of charge displacements in the cathodic direction (*18*). Accordingly, a trace response survived in the inversely oriented sample (Fig. 3C) because a few cathodically responsive PM fragments remain. This lack of a response indicates that the most significant photoelectric response and the maximum charge displacement effect can be elicited from a PM-based photoelectric device in which a highly organized, effective array of PM films is used.

Our studies demonstrate that the preparation of precisely oriented, molecularly regulated bR films can be accomplished through treatment with BS antibodies. We believe that the key to the design of bR-based molecular electronic devices may lie in the ability to control the molecular orientation of bR and the potential applications of this ability to the formation of two-dimensional molecular crystals. Typically, a two-dimensional pixelized image sensor constructed around a PM film (*7*) can serve as a good retina model because pixel size can be minimized while still maintaining equal sensitivity between small pixels. Particularly promising is the extension of this technique to the preparation of three-dimensional crystals of functional proteins, starting with self-assembly of a protein multilayer (*19*) on a highly oriented two-dimensional base. Solid crystals of bR that have a three-dimensionally oriented network of retinal chromophore can be obtained as intelligent materials for incorporation into optoelectronic and nonlinear optical applications.

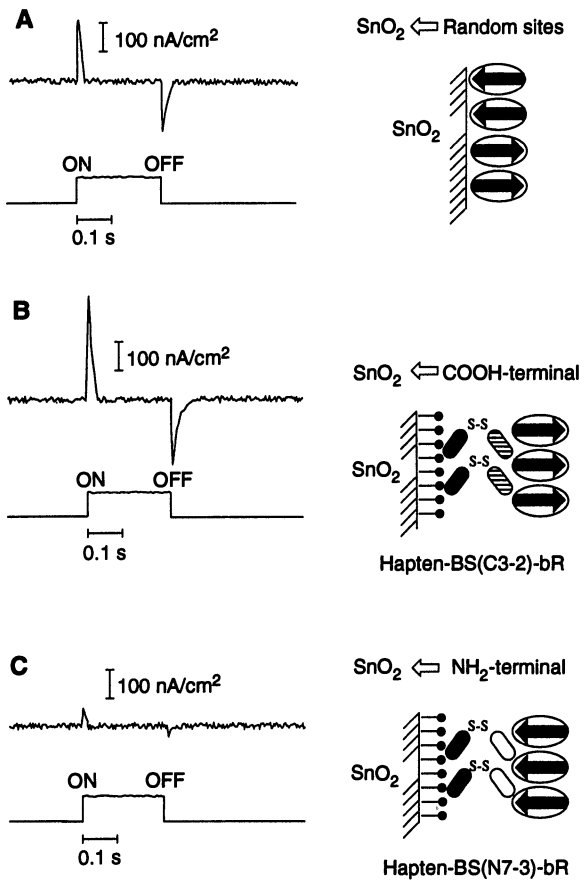

Fig. 3. Comparison of the typical photoelectric response from a sandwich-type photocell comprising junctions of SnO_2 electrode/PM monolayer film/aqueous gel (4% carboxymethyl chitin and 1 M KCl)/Au counter electrode. The SnO_2 electrode (1.8 cm by 2.0 cm) is made of a glass plate bearing a 4500 Å–thick conductive layer of SnO_2 with an electrical resistance of 20 ohm/cm). A small amount of an aqueous electrolyte gel containing 4% carboxymethyl chitin and 1 M KCl (pH 7 to 8) was applied on the PM monolayer film, turned on the SnO_2 electrode and the electrode was sandwiched with a counter-electrode (an Au-sublimated glass plate), using a Teflon ring spacer (thickness, 300 μm). The PM monolayer film (irradiation area, 0.2 cm^2) was irradiated with green light supplied by a 150-W xenon arc lamp in combination with a filter system (Toshiba G55S and IRA-05; transmittance peak 540 nm, half-width 130 nm) that gave an incident intensity of about 10 mW/cm^2. Light excitation of bR caused a charge displacement photocurrent, which responds differentially upon the switching of light irradiation (a time profile is shown). (**A**) Photoelectric response from a monolayer PM film prepared by the LB method, which is randomly oriented. (**B**) An oriented monolayer PM film with the cytoplasmic side facing the SnO_2 electrode. (**C**) An oriented monolayer PM film with the extracellular side facing the SnO_2 electrode. The arrows indicate the orientation of bR along the direction of proton pumping.

REFERENCES AND NOTES

1. R. Henderson and P. N. T. Unwin, *Nature* **257**, 28 (1975); D. Engelman, R. Henderson, A. McLachlan, B. Wallace, *Proc. Natl. Acad. Sci. U.S.A.* **77**, 2023 (1980); R. Henderson *et al.*, *J. Mol. Biol.* **213**, 899 (1990).
2. M. Braiman *et al.*, *Biochemistry* **27**, 8516 (1988); T. Mogi, L. Stern, T. Marti, B. Chao, H. Khorana, *Proc. Natl. Acad. Sci. U.S.A.* **85**, 4148 (1988); H. Otto *et al.*, *ibid.* **86**, 9228 (1989).
3. L. Song, M. A. El-Sayed, J. K. Lanyi, *Science* **261**, 891 (1993).
4. H. Takei, A. Lewis, Z. Chen, I. Nebenzahl, *Appl. Opt.* **30**, 500 (1991); D. Haronian and A. Lewis, *ibid.*, p. 597.
5. R. Birge, *Annu. Rev. Phys. Chem.* **41**, 683 (1990); N. Hampp, D. Bräuchle, D. Oesterhelt, *Biophys. J.* **58**, 83 (1990).
6. T. Miyasaka, K. Koyama, I. Itoh, *Science* **255**, 342 (1992); T. Miyasaka and K. Koyama, *Thin Solid Films* **210/211**, 146 (1992).
7. T. Miyasaka and K. Koyama, *Appl. Opt.* **32**, 6371 (1993).

8. H.-W. Trissl, *Photochem. Photobiol.* **51**, 793 (1990).
9. N. Yamaguchi, Y. Jinbo, M. Arai, K. Koyama, *FEBS Lett.* **324**, 287 (1993).
10. E. Uzgiris and R. D. Kornberg, *Nature* **301**, 125 (1983).
11. Two kinds of peptides were synthesized as antigens to produce monoclonal antibodies to each side of bR. One comprises 18 residues of Gly^{231} to Ser^{248} (COOH-terminal portion of bR) on the cytoplasmic side, the other 9 residues of (pyr)-Glu-1 to Glu-9 (NH_2-terminal portion of bR) on the extracellular side. The two peptides were conjugated to KLH as a carrier protein before being immunized to mice (*9*).
12. M. Brennan, P. F. Davison, H. Paulus, *Science* **229**, 81 (1985).
13. D. Oesterhelt and W. Stoeckenius, *Methods Enzymol.* **31**, 667 (1974).
14. We labeled monoclonal antibody N7-3 with gold particles by mixing colloidal gold solution (~5 nm in diameter; BioCell) with N7-3 in bolax-HCl buffer (pH 9) and adding bovine serum albumin after 10 min. The antibody-gold complex was centrifuged for 40 min, the resultant precipitate was suspended in a small amount of phosphate-buffered saline to form a 1% solution (final concentration, absorbance at 520 nm = 0.1), and the suspension (N7-3–Au conjugate) was used for electron microscopy.
15. We also prepared a randomly oriented sample with a separating layer by transferring a PM-LB monolayer film on an electrode modified with a hapten phospholipid and a BS antibody. The response obtained from this sample decreased by 30% as compared with an LB film directly attached to a substrate.
16. A. McIntosh and F. Boucher, *Biophys. J.* **60**, 1 (1991); A. McIntosh and F. Boucher, *Biochim. Biophys. Acta* **1056**, 149 (1991).
17. We have not detected slow signals that may arise from the proton pumping process.
18. T. Miyasaka and K. Koyama, *Chem. Lett.* **1991**, 1645 (1991).
19. A method for constructing self-assembled protein multilayers has been described by Müller *et al.*, using molecular recognition between avidin and biotin [*Science* **262**, 1706 (1993)].
20. We thank I. Itoh for helpful comments and discussions. We also thank H. Namikawa for technical assistance with antibody techniques and M. Arai with electron microscopy.

18 March 1994; accepted 31 May 1994

Excimers and Exciplexes of Conjugated Polymers

Samson A. Jenekhe* and John A. Osaheni

Observations of intermolecular excimers in several π-conjugated polymers and exciplexes of these polymers with tris(*p*-tolyl)amine are reported. It is shown that the luminescence of conjugated polymer thin films originates from excimer emission and that the generally low quantum yield is the result of self-quenching. Thus, in sufficiently dilute solution, the "single-chain" emission has a quantum yield of unity. Exciplex luminescence and exciplex-mediated charge photogeneration have much higher quantum yields than the excimer-mediated photophysical processes. These results provide a basis for understanding and controlling the photophysics of conjugated polymers in terms of supramolecular structure and morphology.

Conjugated polymers have attracted much research interest in science and technology in the past two decades (*1–5*). Conducting polymers (*1–5*), which are ground-state, charge-transfer complexes of conjugated polymers, are of wide interest as semiconductors and electroactive materials for diverse applications ranging from biosensors, batteries, and loudspeakers to molecular electronic devices (*3–5*). In their pristine form, π-conjugated polymers are of wide interest as third-order nonlinear optical materials for photonic switching devices (*4, 6, 7*) and as optoelectronic materials for light-emitting diodes (*8, 9*), solar cells (*10*), and xerographic photoreceptors (*11*). Exciplexes, which are charge-transfer complexes that are stable only in the excited state, are important materials that have only recently begun to be explored in conjugated polymers (*12, 13*). Although much theoretical and experimental work has been done on the photophysics of conjugated polymers (*14–18*), including the nature of the excited states, the origin of luminescence, and the nature of charge photogeneration, these photophysical processes in conjugated polymers remain poorly understood and controversial (*14–18*).

One common way in which excimers (*19–27*) are formed is by interaction of an excited chromophore $^1A^*$ with an unexcited chromophore ^1A: $^1A^* + {}^1A \rightleftharpoons {}^1(AA)^*$. Such an excited-state complex is stable as a result of resonance contributions from exciton and charge-transfer configurations: $^1(A^*A) \leftrightarrow {}^1(AA^*) \leftrightarrow {}^1(A^-A^+) \leftrightarrow {}^1(A^+A^-)$. The corresponding excimer wave function is (*21, 23*).

$$\Psi_{excimer} = c_1[\Psi(A^*A) + \Psi(AA^*)] + c_2[\Psi(A^-A^+) + \Psi(A^+A^-)]$$

The ratio c_1/c_2 and hence the relative contributions from exciton and charge transfer may vary for different materials. Singlet exciplexes are formed similarly but from two distinct chromophores A (acceptor) and D (donor) [either A or D is excited, that is, $^1A^* + {}^1D$ or $^1A + {}^1D^* \rightarrow {}^1(A^{\cdot-}D^{\cdot+})$], and are similarly stabilized (*21, 24*) [$^1(A^*D) \leftrightarrow {}^1(AD^*) \leftrightarrow {}^1(A^{\cdot-}D^{\cdot+})$].

Studies (*19–27*) of excimers and exciplexes in small molecules have shown that their basic supramolecular structures are cofacial sandwich-type configurations with interplanar distances of 3 to 4 Å. Interestingly, π-conjugated polymers are generally stiff chain molecules with relatively planar geometries and very strong intermolecular interactions, leading to cofacial chain packing in the solid state (*2, 3, 28, 29*). Intermolecular distances of 3.3 to 3.6 Å in sandwich-type cofacial packing have been determined by x-ray diffraction and by computational modeling of the supramolecular structure and morphology of many π-conjugated polymers (*28, 29*). It is therefore reasonable to expect that excimers might efficiently form in excited π-conjugated polymers because the materials are already configured into potential excimer-forming sandwich-type supramolecular structures.

We report the formation of intermolecular excimers by a series of π-conjugated polybenzobisthiazoles (**1**), polybenzobisoxazole (**2a**), and poly(benzimidazobenzophenanthroline ladder) (**3**) (Fig. 1). We also report the formation of intermolecular exciplexes between these polymers and tris(*p*-tolyl) amine (**4**). The formation and properties of excimers $^1(AA)^*$ and exciplexes $^1(A^{\cdot-}D^{\cdot+})^*$, where A is a conjugated polymer chromophore and D is **4**, were investigated by steady-state and time-resolved fluorescence spectroscopy, picosecond transient absorption spectroscopy, and charge photogeneration in xerographic photoinduced discharge experiments. Dilute and concentrated fluid and solid solutions as well as thin films of these rigid chain polymers were investigated (*30*).

All photophysical measurements were done at room temperature. Optical absorption and excitation spectra of 10^{-7} to 10^{-3} M fluid solutions in methanesulfonic acid (MSA) and 10^{-3} to 12 M solid solutions in poly(benzobisthiazole decamethylene) were obtained (*30*). Steady-state photoluminescence (PL) measurements were made on the same fluid and solid solutions as well as on thin films of the polymers. We measured the PL quantum yield Φ_f by comparing the integration of the emission spectrum of a sample to that of a standard of known Φ_f under identical optical conditions (*25, 31, 32*). A 10^{-6} M quinine sulfate solution (0.1 N in H_2SO_4, Φ_f = 55%) (*31*) and a thin film of ~10^{-3} M 9,10-diphenylanthracene in poly(methyl methacrylate) (Φ_f = 83%) (*32*) were used as fluorophore standards for fluid solutions and thin films, respectively. We made picosecond time-resolved PL decay measurements using the time-correlated

Department of Chemical Engineering and Center for Photoinduced Charge Transfer, University of Rochester, Rochester, NY 14627, USA.

*To whom correspondence should be addressed.